Journal of Nuclear Materials 402 (2010) 81–86

Contents lists available at ScienceDirect

Journal of Nuclear Materials

journal homepage: www.elsevier.com/locate/jnucmat

Synthesis and characterization of zirconia–magnesia inert matrix fuel: Plutonium studies

Kiel Holliday [a,*], Thomas Hartmann [a], Sean R. Mulcahy [b], Ken Czerwinski [a]

[a] Harry Reid Center for Environmental Studies, University of Nevada, Las Vegas, United States
[b] Department of Geoscience, University of Nevada, Las Vegas, United States

ARTICLE INFO

Article history:
Received 8 February 2010
Accepted 30 April 2010

ABSTRACT

This study uses a precipitation method to synthesize zirconia–magnesia inert matrix fuel containing plutonium oxide as the fissile material and erbium oxide as a burnable poison. X-ray diffraction, secondary electron microscopy with energy dispersive spectroscopy, optical microscopy, and electron probe microanalysis were used to determine phases present, phase mixing, microstructure, phase stoichiometry, and elemental distributions throughout the samples. A large range of magnesium to zirconium oxides as well as different concentrations of plutonium and erbium oxides was studied. It was found that it was possible to synthesize a two phase material consisting of a pure MgO (periclase) phase and a cubic zirconia phase which incorporated all of the plutonium and erbium as well as a small amount of the magnesium oxides. This information will be used to understand the dissolution behavior and properties of this material in conditions relevant to an advanced nuclear fuel cycle.

1. Introduction

There has been a recent resurgence of interest in different oxide fuel types as potential advanced burner fuel for nuclear energy systems, often highlighting the role of transuranic elements as the fissile component. Inert fuel matrices have the advantage of burning plutonium and other transuranic elements from the fuel cycle without the production of higher actinides [1–3]. Competitive methods for plutonium destruction include mixed oxide fuels that contain uranium. This can increase proliferation resistance by altering plutonium isotopics, but does not significantly reduce the radiotoxicity of the plutonium [4]. Neutronic calculations indicate that up to 83% of the loaded plutonium can be burnt in a uranium free fuel in the thermal spectrum [5,6]. Inert matrix fuel would simultaneously reduce radiotoxicity and proliferation risk in spent fuel. The fissile material in the fuel must be volumetrically diluted by an inert matrix, which is by definition neutron transparent. It must also be compatible with reactor materials such as cladding and coolant. Additionally, a new fuel must be proliferation resistant, correspond to current safeguards and environmental safety, be economically viable, and refuel on the current time scale [1,7].

One of the most widely studied candidate inert matrix materials is cubic zirconia. It is radiation tolerant and compatible with reactor materials [2,3,8–12]. It fully incorporates the fissile material and burnable poisons. Cubic zirconia, however, does not conduct heat as well as current fuels resulting in unacceptably high centerline temperatures. To compensate for this, a second phase such as MgO may be added to improve thermal diffusivity and thermal conductivity [13,14]. Unfortunately, pure MgO cannot be used as an inert matrix fuel, as it undergoes hydrolysis and subsequent swelling in the event of a cladding failure [13,15].

Under static 300 °C water it has been shown that the addition of ZrO_2 has an exponential decrease in the corrosion rate of the zirconia–magnesia material [15]. The thermal conductivity of the composite is greater than that of UO_2 making it suitable for current reactor safety guidelines with respect to centerline temperatures [16]. Further study of this material is needed to better understand the chemistry of the zirconia–magnesia matrix containing a fissile component and any burnable poisons. Previous studies used conventional milling and sintering techniques to synthesize zirconia–magnesia containing PuO_2 and Er_2O_3, but this resulted in the formation of a third phase of plutonium oxide microspheres instead of incorporating into the zirconia as desired [17,18]. This study aims at synthesizing a dual phase ceramic that has the fissile material and burnable poison incorporated into the zirconia phase. X-ray powder diffraction, optical and secondary electron microscopy, and electron probe microanalysis are used to determine bulk concentrations, phases present, phase mixing, and phase composition. These studies are a basis for future work on dissolution properties of the material in conditions relevant to an advanced nuclear fuel cycle. Previous work with cerium and uranium as a plutonium homolog is the foundation for comparison [19,20], while this work presents the characterization of the material using plutonium as the fissile component. Future studies will be aimed at the dissolu-

---

* Corresponding author.
E-mail address: holliday.kiel@gmail.com (K. Holliday).

0022-3115/$ - see front matter © 2010 Elsevier B.V. All rights reserved.
doi:10.1016/j.jnucmat.2010.04.026

tion behavior of this material in reactor, reprocessing, and repository environments.

2. Experimental

2.1. Ceramic fabrication

A wet chemical precipitation method was chosen for ceramic fabrication because less severe sintering temperatures and times were required to produce a homogenous sample. Concentrated aqueous nitrate or chloride salt solutions of zirconium ($ZrO(NO_3)_2$), magnesium ($MgCl_2$), and erbium ($Er(NO_3)_3$) were prepared. A 4 M nitric acid solution was used as the source of plutonium (13.5 mM). These solutions were mixed in appropriate proportions and the metals coprecipitated with an ammonia hydroxide solution saturated with ammonium oxalate. All chemicals are reagent grade and were purchased from Alpha Aesar with the exception of plutonium, which was obtained from Isotope Productions Laboratory. The precipitate was filtered and washed with purified water and acetone to remove excess ammonia. Due to the high solubility of magnesium, however, it was found that an elevated proportion of the magnesium was contained in the filtrate. This became evident in this study due to the reduced product mass in this work; several grams in previous efforts to around 100 mg in this study [19,20]. As a result the precipitate was not filtered but evaporated to dryness to synthesize material with a high magnesia component. The resulting oxy-hydroxide precipitate was dried in an oven at 100 °C for 24 h. The dry precipitate was then ground by mortar and pestle to a powder before being calcined at 700 °C overnight in air to convert it to the oxide. The oxide powder was cold pressed to 500–600 MPa with a SPEX Carver hydraulic press in a SPEX 5 mm die to produce green pellets. These pellets were placed on Pt foil in an alumina boat and were then sintered at 1600 °C in a Reetz LORA tube furnace for 10 h under argon atmosphere.

Plutonium oxide content was varied to determine the solubility of plutonium within the zirconia phase. Neutronic calculations have shown an optimal volume ratio of burnable poison to be half that of the fissile phase [21]. The erbium oxide content was therefore varied from half of the plutonium content to equal to that of plutonium in order to explore the relevant compositional range. The inert matrix was composed of zirconium oxide and magnesium oxide and was varied to explore the range of compositions. The bulk concentrations used to synthesize the pellets in this study are listed in Table 1.

2.2. X-ray diffraction (XRD)

Sintered pellets were ground to a powder and approximately 10 mg was spread in a thin layer over a low-background sample holder (single crystal silicon wafer) with the aid of methanol. X-ray diffraction patterns were collected on a Bruker D8 Advance diffractometer, which uses a Cu anode and a Johansson-type primary monochromator (wavelength $K\alpha_1$ at 0.1540598 nm). Patterns were taken using 40 mV and 40 mA from 10 to 120°2θ with a step size of 0.01°2θ and 4 s per step. Phases were identified using Bruker-AXS EVA. Bruker-AXS TOPAS3 was then used to fit the diffracted intensities and to perform least-square and Rietveld analysis. Structure input parameters were taken from Inorganic Crystal Structure Database. Instrument parameter inputs were as follows: primary radius (mm) 435, secondary radius (mm) 435, receiving slit width (mm) 0.1, divergence angle (°) 1, filament length (mm) 12, sample length (mm) 8, receiving slit length (mm) 12, secondary sollers (°) 2.3, and Lorenz polarization factor was set to 26.6.

Table 1
Sample composition by mass as calculated from phase quantity (Rietveld analysis) and phase stoichiometry (energy dispersive spectroscopy) (not normalized to 100%).

Sample #	ZrO_2%	MgO%	PuO_2%	$ErO_{1.5}$%
1	71	3.0	16	9.0
2	75	11	7.5	7.5
3	67	14	9.8	8.2
4	58	20	12	9.8
5	42	50	4.7	2.4
6	23	72	3.5	2.0
7	16	79	3.4	1.8

2.3. Microscopy and electron probe microanalysis

Pellets were vacuum mounted with Struers Epofix resin. Sample mounts were then ground and polished to a mirrored finish (1 μm) using a Struers TegraPol-15. Pellets were imaged using a Leica 2500P microscope with a DFC 295 camera. Images were analyzed using Leica Application Suite 3.3.0. After imaging the pellets, they were carbon coated and analyzed with a JEOL JXA 8900R electron probe microanalyzer. Elemental mapping was done over areas up to several mm^2 at 15 keV and 100 nA. A JEOL 5600 scanning electron microscope equipped with energy dispersive spectroscopy was used to evaluate microstructure evolution and to determine stoichiometry of phases for plutonium containing samples. Samples were analyzed at 20 keV, working distance of 20 mm, and a spot size of 30.

3. Results and discussion

3.1. Synthesis

One of the main goals of this study was to synthesize a two phase inert matrix fuel of periclase (a pure MgO phase) and cubic zirconia, which would incorporate the fissile material and burnable poison through isomorphic substitution. This was previously not possible through mixing of the oxide powders and subsequent pressing and sintering due to plutonium oxide forming a third phase not incorporated into the zirconia [17,18]. Because of this

Fig. 1. Picture of sintered plutonium containing zirconia–magnesia inert matrix fuel ($Zr_{0.76}Mg_{0.10}Pu_{0.078}Er_{0.062}O_{1.9}$).

a precipitation method was employed for this study. This allows for more complete mixing and has been shown to form solid solutions at less extreme temperatures and times during sintering [19]. The current study was successful in synthesizing a two phase inert matrix fuel as predicted by previous homolog studies [20]. This method produced pellets >95% theoretical density based on mass and a geometric measure of volume (Fig. 1).

A notable difference between the plutonium studies presented here and previous studies using uranium and cerium is in the amount of material produced in each batch. Previous efforts were performed by precipitating out tens of grams to form several pellets [19,20]. Due to the high activity of plutonium the amount of material precipitated in a batch was reduced to 100 mg. Because of this, the small differences in solubility of the cations after precipitation manifests as fluctuations in the concentrations in the solid. Most notably is the high solubility of magnesium resulting in a drop in magnesium oxide concentration in the solid. To avoid this loss the precipitate was not filtered but heated to dryness, then calcined to synthesize the samples with magnesium oxide concentrations higher than 25 wt.% (Table 1). Since the nitrate and chloride counter ions are volatile it was possible to avoid any loss of material without the incorporation of impurities. In a larger scale production this should not be necessary as the differences in solubility are insignificant when compared to the amount of material that is produced.

3.2. X-ray diffraction

X-ray diffraction was used to identify and quantify crystalline phases present in the inert matrix fuel. It was found in the sample with the lowest MgO concentration (3 wt.% MgO) only a cubic zirconia phase was present, indicating that all other cations were dissolved in the zirconia lattice through isomorphic substitution (Fig. 2). Once the MgO concentration is increased to 11 wt.% it exceeds the solubility limit for isomorphic substitution in cubic zirconia and precipitates as cubic MgO (periclase) (Fig. 3). This is expected as the solubility limit for MgO in zirconia under similar conditions was determined in previous studies to be 6.9% (wt/wt) [19]. This two phase mixture of zirconia and periclase was found in all samples with more than 7 wt.% MgO with a maximum periclase phase for this sample set being 77 wt.% (Fig. 4).

The lattice parameter for the periclase phase remains consistent and is independent of the concentration of other elements suggesting that it is pure MgO and no other elements are incorporated into

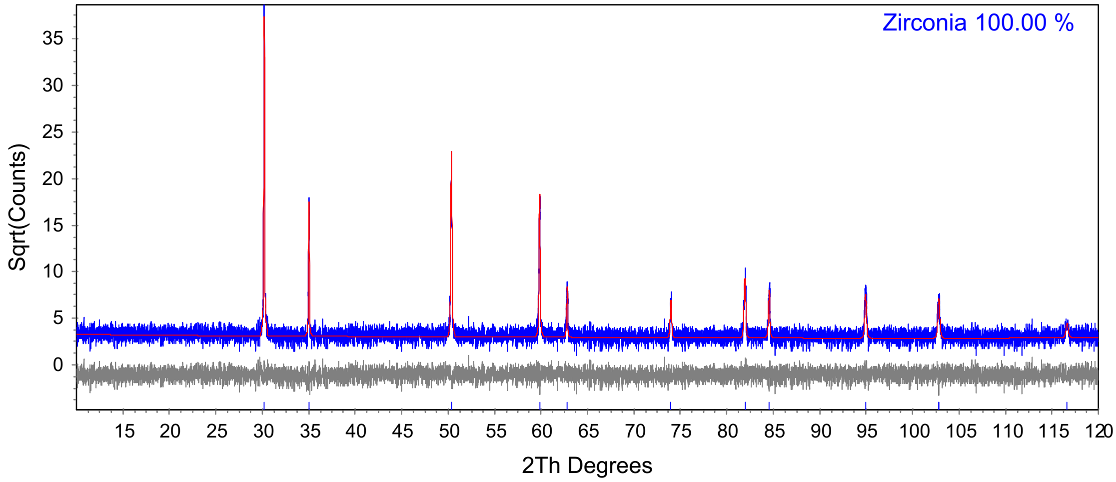

Fig. 2. X-ray diffraction pattern of $Zr_{0.76}Mg_{0.10}Pu_{0.078}Er_{0.062}O_{1.9}$ (blue) with fit (red) and difference curve (grey). (For interpretation of the references to colour in this figure legend, the reader is referred to the web version of this article.)

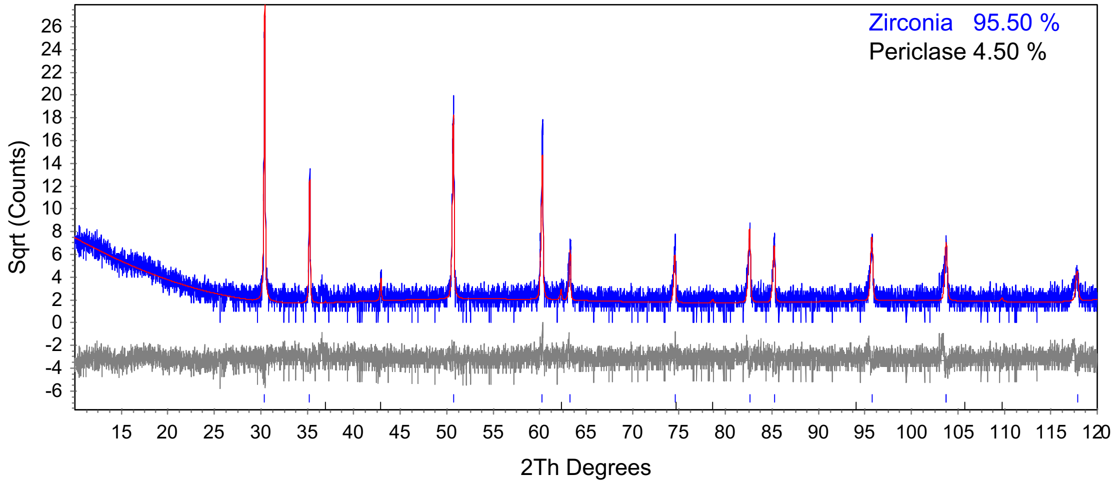

Fig. 3. X-ray diffraction pattern of $Zr_{0.64}Mg_{0.29}Pu_{0.029}Er_{0.041}O_{1.7}$ (blue) with fit (red) and difference curve (grey). (For interpretation of the references to colour in this figure legend, the reader is referred to the web version of this article.)

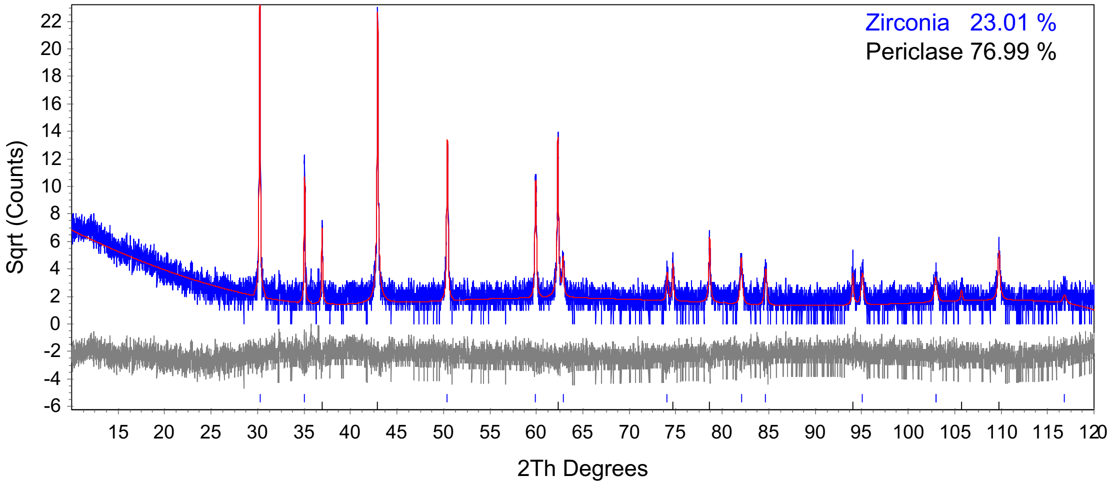

Fig. 4. X-ray diffraction pattern of $Zr_{0.061}Mg_{0.93}Pu_{0.0059}Er_{0.0045}O_{1.1}$ (blue) with fit (red) and difference curve (grey). (For interpretation of the references to colour in this figure legend, the reader is referred to the web version of this article.)

Table 2
Phases present, quantity, and lattice parameters as determined by XRD along with phase stoichiometry as determined by SEM/EDS.

Composition of samples #	Phases present	Lattice parameter (nm)	Phase stoichiometry	Quantity (wt/wt)
1: $Zr_{0.76}Mg_{0.10}Pu_{0.078}Er_{0.062}O_{1.9}$	ZrO_2 (Fm-3 m)	0.51215(15)	$Zr_{0.76}Mg_{0.098}Pu_{0.078}Er_{0.062}O_{1.9}$	100
2: $Zr_{0.64}Mg_{0.29}Pu_{0.029}Er_{0.041}O_{1.7}$	ZrO_2 (Fm-3 m)	0.50905(19)	$Zr_{0.79}Mg_{0.12}Pu_{0.036}Er_{0.051}O_{1.9}$	93.3
	MgO (Fm-3 m)	0.42126(17)	MgO	6.7
3: $Zr_{0.56}Mg_{0.36}Pu_{0.037}Er_{0.044}O_{1.6}$	ZrO_2 (Fm-3 m)	0.50973(16)	$Zr_{0.79}Mg_{0.098}Pu_{0.052}Er_{0.061}O_{1.9}$	88.7
	MgO (Fm-3 m)	0.42133(13)	MgO	11.3
4: $Zr_{0.44}Mg_{0.47}Pu_{0.042}Er_{0.048}O_{1.5}$	ZrO_2 (Fm-3 m)	0.51086(13)	$Zr_{0.75}Mg_{0.098}Pu_{0.073}Er_{0.082}O_{1.9}$	82.2
	MgO (Fm-3 m)	0.42129(11)	MgO	17.8
5: $Zr_{0.21}Mg_{0.77}Pu_{0.011}Er_{0.0078}O_{1.2}$	ZrO_2 (Fm-3 m)	0.50984(15)	$Zr_{0.82}Mg_{0.11}Pu_{0.042}Er_{0.030}O_{1.9}$	48.2
	MgO (Fm-3 m)	0.42110(12)	MgO	51.84
6: $Zr_{0.093}Mg_{0.89}Pu_{0.0065}Er_{0.0052}O_{1.1}$	ZrO_2 (Fm-3 m)	0.51042(21)	$Zr_{0.80}Mg_{0.097}Pu_{0.056}Er_{0.046}O_{1.9}$	29.2
	MgO (Fm-3 m)	0.42169(17)	MgO	70.8
7: $Zr_{0.061}Mg_{0.93}Pu_{0.0059}Er_{0.0045}O_{1.1}$	ZrO_2 (Fm-3 m)	0.51160(20)	$Zr_{0.77}Mg_{0.10}Pu_{0.076}Er_{0.058}O_{1.9}$	21.5
	MgO (Fm-3 m)	0.42117(16)	MgO	78.5

the lattice (Table 2) above trace amounts. The lattice parameter for the zirconia increases with increasing plutonium and erbium content indicating that plutonium and erbium is isomorphically substituted into the zirconia lattice as shown in Table 2. This is further evidence that a third plutonium or erbium rich phase is not present, even as an amorphous material. The zirconium oxide concentration of the total pellet was decreased as low as 16 wt.% with no evidence of third phase formation (Fig. 4). This indicates the solubility limit for plutonium and erbium within the zirconia phase is high enough to accommodate a wide range of zirconia to magnesia ratios. The solubility limit of plutonium and erbium in zirconia is further discussed in the microscopy section. The quantities of each phase, lattice parameters, and space group as determined by Rietveld refinement and least squares fitting are listed in Table 2.

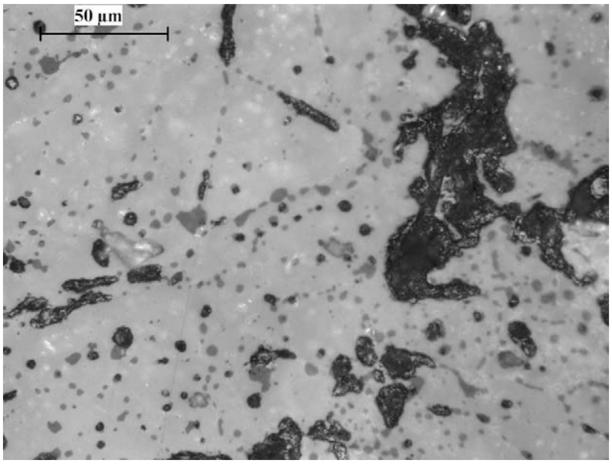

Fig. 5. Optical microscopy image at 500× magnification of $Zr_{0.64}Mg_{0.29}Pu_{0.029}Er_{0.041}O_{1.7}$.

3.3. Microscopy and electron probe microanalysis

Optical microscopy proved to be a useful tool in visualizing phase mixing and pore space. It was shown that the periclase phase appeared as a dark gray while pore space was black and the zirconia phase was identified as the light grey phase. It was observed that even at periclase phase concentrations as low as 4.5 wt.% the phase is still evenly distributed throughout the sample with an intimate phase mixing (Fig. 5). This intimate mixing is evident through all samples and shows an interconnected periclase phase at 50 wt.% MgO (Fig. 6). This interconnected periclase phase will allow thermal diffusivity from the center of the pellet to the peripheral because of its superior heat transfer properties, thereby lowering the centerline temperature of the fuel.

Electron probe microanalysis was used to scan an area of the polished surface to map relative concentrations of zirconium, magnesium, plutonium, erbium, and oxygen. In this way it is possible to identify elements that have affinity for the same phase and

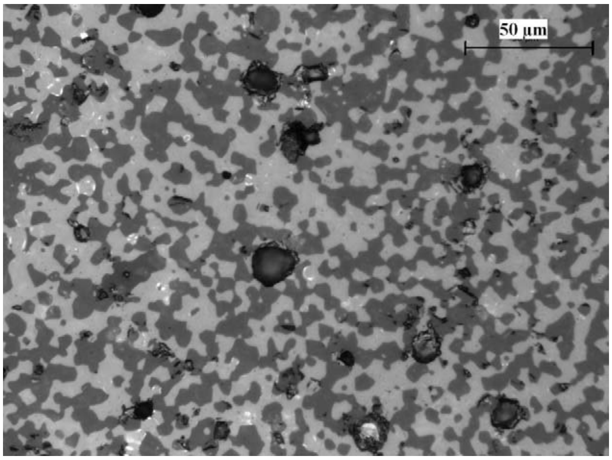

Fig. 6. Optical microscopy image at 500× magnification of $Zr_{0.21}Mg_{0.77}Pu_{0.011}Er_{0.0078}O_{1.2}$.

those that are exclusive to a phase as previously identified by XRD. All pellets examined exhibited the same characteristics. The periclase phase was shown to have no affinity for any elements other than magnesium and oxygen, consistent with the XRD results. This is shown in Fig. 7a by the areas of high Mg concentration (brighter) that correspond to areas showing no concentration (black) of any other element (Fig. 7b–d) as previously suggested by the constant lattice parameter of the periclase based on XRD (Table 2). The zirconia phase incorporates a small amount of magnesium into the lattice as indicated by a faint image of the zirconia phase in a map of magnesium concentration (Fig. 7a). All of the zirconium, plutonium, and erbium, are evenly distributed throughout the zirconia phase as shown by the consistent amount of each element throughout the phase and identical maps of elemental distribution (Fig. 7b–d). This will simplify modeling of the material as only two phases need to be considered and is an improvement over previous attempts at synthesizing a plutonium containing zirconia–magnesia inert matrix fuel which resulted in a three phase material [17,18]. This method also verified that both phases have a high degree of homogeneity in each phase.

A secondary electron microscope equipped with an energy dispersive spectrometer was used to take semi-quantitative measurements in small volumes ($\sim$2–5 μm^3) in an effort to quantify the elements present in each phase. This method confirmed that the periclase phase is pure MgO. The zirconia phase is more complicated, as it incorporates all cations involved by isomorphic substitution. Magnesium was found in the zirconia phase at a constant 3–4 wt.% over all samples which defines the limit of isomorphic substitution of magnesium in the zirconia phase. This is within the range of 3–7 wt.% established by similar studies [19,20]. There was no limit found for plutonium or erbium within the range of samples synthesized in this study. Plutonium content within the zirconia phase was as high as 16 wt.% and erbium content reached as high as 12 wt.% within the zirconia phase. This allows for loading the needed fissile material even at low concentrations of zirconium oxide resulting in high concentration of plutonium and erbium within the zirconia phase. A complete list of quantitative

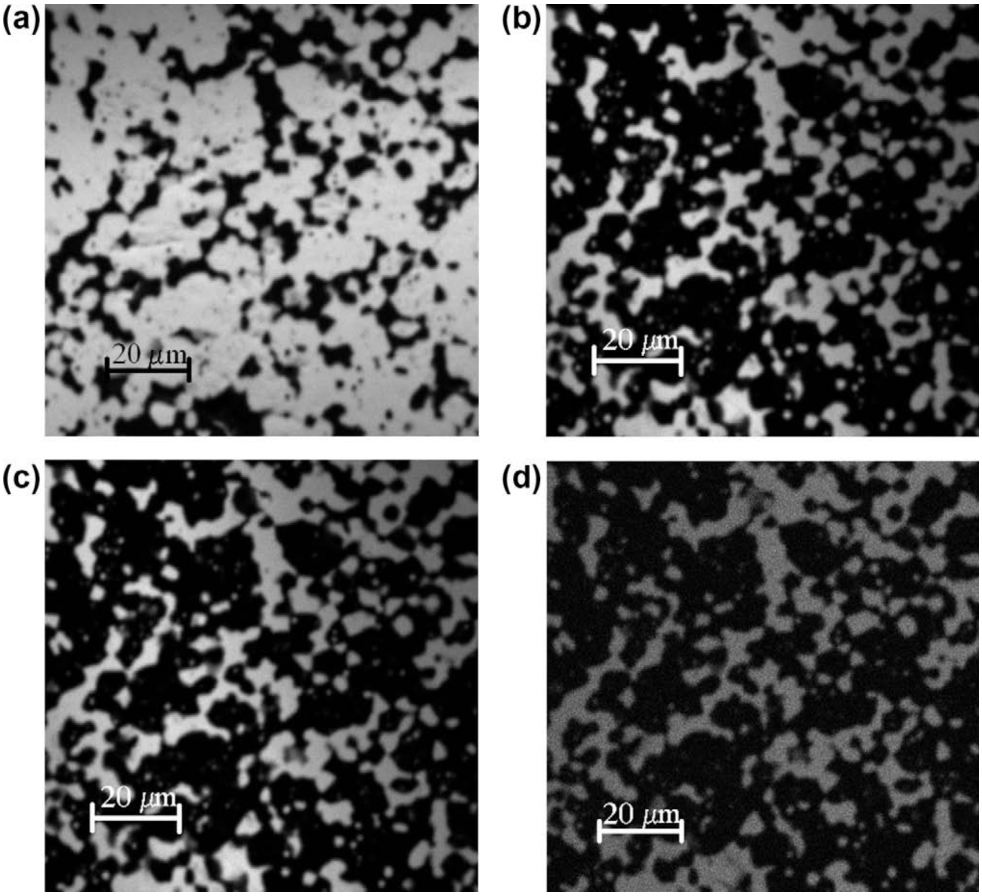

Fig. 7. Elemental mapping over 125 × 125 μm area by electron probe microanalysis of $Zr_{0.093}Mg_{0.89}Pu_{0.0065}Er_{0.0052}O_{1.1}$. (a) Magnesium Kα map, (b) zirconium Lα map, (c) plutonium Mα map, and (d) erbium Lα map.

results and stoichiometry of each phase as determined by energy dispersive spectrometry is listed in Table 2.

4. Conclusions

A zirconia–magnesia inert matrix fuel containing plutonium oxide as the fissile material and erbium oxide as a burnable poison was successfully synthesized as a dual phase ceramic using a precipitation method over a range of compositions. The precipitation method allows suitable chemical mixing to produce the two phase material. This product was characterized by XRD in an effort to identify and quantify crystalline phases present. It was shown in most samples that the material consisted of cubic zirconia and cubic MgO (periclase). Optical microscopy was used to visualize phase mixing, microstructure, and pore space. Electron probe microanalysis was used to map elemental concentrations over wide areas. This proved the homogeneity of each phase and confirmed that plutonium and erbium are incorporated into the zirconia phase resulting in a solid solution. This will simplify modeling and has not previously been achieved. Secondary electron microscopy equipped with energy dispersive spectroscopy was used to (semi-quantitatively) determine the stoichiometry of each phase. It was determined that the periclase phase was pure MgO. This will allow it to retain its heat transfer properties, specifically thermal diffusivity and thermal conductivity. The periclase phase was found to be interconnected, facilitating thermal diffusivity away from the center of the pellet. This is a crucial property that greatly improves the utility of the examined inert matrix material as a potential fuel to burn plutonium. Analysis of the zirconia phase shows a presence of all cations involved to different concentrations. Magnesium is incorporated into the zirconia at 3–4 wt.% which defines the limit of isomorphic substitution for magnesium in zirconia under these conditions. The solubility limits of plutonium and erbium in zirconia were not reached, however the highest concentration of plutonium and erbium found in the zirconia were 16 and 12 wt.%, respectively. This high solubility limit will allow fissile material to be loaded into the fuel even at low concentrations of zirconium oxide. These studies are aimed at understanding the material for future dissolution studies in conditions of interest to an advanced fuel cycle.

Acknowledgements

This project was funded under the UNLV Transmutation Research Program administered by the Harry Reid Center for Environmental Studies under the auspices of the US Department of Energy, Office of Nuclear Energy (Cooperative Agreement No. DE-FG07-01AL67358).

References

[1] W.J. Carmack, M. Todosow, M.K. Meyer, K.O. Pasamehmetoglu, J. Nucl. Mater. 352 (2006) 276–284.
[2] R. Chawla, R.J.M. Konings, Prog. Nucl. Energy 38 (2001) 455–458.
[3] G. Ledergerber, C. Degueldre, P. Heimgartner, M.A. Pouchon, U. Kasemeyer, Prog. Nucl. Energy 38 (2001) 301–308.
[4] A. Shelley, H. Akie, H. Takano, H. Sekimoto, Prog. Nucl. Energy 38 (2001) 439–442.
[5] C. Lombardi, A. Mazzola, Ann. Nucl. Energy 23 (1996) 1117–1126.
[6] C. Lombardi, A. Mazzola, E. Padovani, M.E. Ricotti, J. Nucl. Mater. 274 (1999) 181–188.
[7] C. Degueldre, J.M. Paratte, J. Nucl. Mater. 274 (1999) 1–6.
[8] G. Curran, W. Rattray, K.R. Czerwinski, Radiochim. Acta 91 (2003) 203–209.
[9] G. Curran, Y. Sevestre, W. Rattray, P. Allen, K.R. Czerwinski, J. Nucl. Mater. 323 (2003) 41–48.
[10] C. Degueldre, S. Conradson, Appl. Phys. A: Mater. Sci. Process. 73 (2001) 489–494.
[11] N. Kamel, H. Ait-Amar, M. Taouinet, C. Benazzouz, Z. Kamel, H. Fodil-Cherif, S. Telmoune, R. Slimani, A. Zahri, D. Sahel, Prog. Nucl. Energy 48 (2006) 70–84.
[12] F. Vettraino, G. Magnani, T. La Torretta, E. Marmo, S. Coelli, L. Luzzi, P. Ossi, G. Zappa, J. Nucl. Mater. 274 (1999) 23–33.
[13] P. Medvedev, Dissertation, Texas A&M University, 2004.
[14] C. Ronchi, J.P. Ottaviani, C. Degueldre, R. Calabrese, J. Nucl. Mater. 320 (2003) 54–65.
[15] P.G. Medvedev, S.M. Frank, T.P. O'Holleran, M.K. Meyer, J. Nucl. Mater. 342 (2005) 48–62.
[16] P.G. Medvedev, M.J. Lambregts, M.K. Meyer, J. Nucl. Mater. 349 (2006) 167–177.
[17] P.G. Medvedev, J.F. Jue, S.M. Frank, M.K. Meyer, J. Nucl. Mater. 352 (2006) 318–323.
[18] P.G. Medvedev, J.F. Jue, S.M. Frank, Trans. Am. Nucl. Soc. 94 (2006) 827–828.
[19] K. Holliday, T. Hartmann, K. Czerwinski, J. Nucl. Mater. 392 (2009) 487–493.
[20] K. Holliday, T. Hartmann, F. Poineau, J.R. Kennedy, K. Czerwinski, J. Nucl. Mater. 393 (2009) 224–229.
[21] E. Fridman, E. Shwageraus, A. Galperin, Nucl. Technol. 157 (2) (2007) 157–176.